

## A shallow scattering layer: High-resolution acoustic analysis of nocturnal vertical migration from the seabed

Keli Kringel<sup>1</sup>

School of Oceanography, Box 357940, University of Washington, Seattle, Washington 98195

Peter A. Jumars<sup>2</sup>

Darling Marine Center, University of Maine, 193 Clark's Cove Road, Walpole, Maine 04573

D.V. Holliday

BAE SYSTEMS, 4669 Murphy Canyon Road, Suite 102, San Diego, California 92123

### Abstract

Using bottom-mounted, high-frequency, inverted echo sounders (the Tracor acoustic profiling system) to examine acoustic backscattering every 2 min in 50-cm range bins above the seabed, we recorded strong, remarkably regular, nightly migrations of organisms from  $\leq 0.5$  m above the seabed to the upper pelagic layers over a period of 6 d in July–August 1995. Population migration speeds on ascent versus descent (mean  $\pm 1$  SD) were not significantly different when estimated from the mode (or leading/trailing edge) of the population and were  $0.59 \pm 0.24$  cm s<sup>-1</sup> in ascent ( $0.96 \pm 0.25$  cm s<sup>-1</sup> leading edge) and  $0.67 \pm 0.13$  cm s<sup>-1</sup> on descent ( $0.78 \pm 0.14$  cm s<sup>-1</sup> trailing edge). The SD in start times of the ascent over the six nights was only 3 min, and that in the times of the completion of the descent was 7 min. Emergence began after and reentry was completed before downwelling irradiance at photosynthetically active wavelengths 1 m above bottom reached  $0.5 \times 10^{-6}$   $\mu\text{mol quanta cm}^{-2} \text{s}^{-1}$ . Migrants increased column scattering strength at 265 kHz by a factor of 14. Emergence-trap samples and nighttime plankton tows suggested that the migrating population was dominated by mysids, mostly *Neomysis kadiakensis*. Our acoustic results suggest that emergence is much more prevalent and important in coastal and estuarine environments than trapping and net sampling can reveal and hence that this important component of benthic-pelagic coupling requires additional attention both in measurements and in theoretical treatments.

During August and September 1995, we conducted experiments in West Sound, Orcas Island, Washington, using the benthic acoustic monitoring system (BAMS) developed at the Applied Physics Laboratory of the University of Washington. It is a bottom-mounted, radially scanning sonar designed to record high-frequency scattering from the seafloor (Jackson and Briggs 1992). A goal of the experiments was to test by manipulation of local abundances the hypothesis (Jumars et al. 1996) that benthic animals or their biogenic modifications of sediments could be detected in sound scattered from the seabed (Self et al. 2001). During the study, we also deployed an autonomous, multifrequency sonar unit, the Tracor acoustic profiling system (TAPS), nearby

in a bottom-mounted, upward-looking “sounder” mode. The deployment of the TAPS was an opportunistic field test during instrument development, not a formal part of the experiment. For a period of 5.89 d in late July and early August, we recorded values of acoustic volume backscattering strength ( $S_v$ ) from the 22 m of water column directly above it with 0.5-m vertical and 2-min temporal resolution. A strong nightly increase originated at or near the seafloor of the bay. This clear signal and the high temporal and spatial resolution of the measurements allowed us to detail a remarkably regular pattern of population migrations from the bottom.

Diel migrations of marine organisms are well documented in the open sea—for example, the migration of the deep scattering layer (Farquhar 1970). Considerably less attention has been given to day-night changes in acoustic scattering in shallow coastal waters. Organisms of many taxa, however, make nightly excursions from the bottom into the water column in concert with both solar and lunar cycles of illumination (e.g., Alldredge and King 1980). A multifrequency, bottom-moored, inverted echo sounder has been used at least once before to study vertical migration but in a lake and with the transducer mounted high above the bottom (Trevorrow and Tanaka 1997). The novelty of our study lies in high spatial and temporal resolution of the acoustic data that allow direct estimation of times and speeds of the daily migration and our ability to census a large fraction of the total water column to resolve the broader influence of emergence.

<sup>1</sup> Current address: SatMetrix Systems, 100 View St., Suite 200, Mountain View, CA 94041.

<sup>2</sup> Corresponding author (jumars@maine.edu).

### Acknowledgments

We thank Robert F. L. (Liko) Self, Charles Greenlaw, Duncan McGehee, Larry Howell, Larry Deuser, Steve Beck, David Lockett, and Monty Northrup for help through the various phases of this project. We also extend our appreciation to Mr. and Mrs. John Gorton, who provided access to their dock and space in their home on Orcas Island for the “dry end” of the data logging system and Tom Duda for help with intensive sampling efforts. We thank A. O. Dennis Willows, Director of the Friday Harbor Laboratories, for small-boat use and for lab space ashore. Financial support came from the U.S. Office of Naval Research. Mike Landry and two anonymous reviewers provided very helpful comments for revision.

Using emergence-trap samples collected in the study region both during and after the acoustic sampling, plankton tows taken afterward, and the results of a multifrequency inverse calculation to process the TAPS data (Holliday 1977; Greenlaw and Johnson 1983; Holliday 1993; McGehee et al. 1998), we investigated the cause of the large acoustic scattering changes seen at night in West Sound. Emergence-trap samples were consistent with size spectra estimated by inverting volume scattering measurements made with the acoustic sensor. On the basis of both the acoustics and specimens captured in traps and plankton nets, we conclude that the dominant cause of the observed nocturnal increases in acoustic scattering was migration of the mysid *Neomysis kadakensis*. Our analysis demonstrates that high-frequency acoustics guiding deliberately timed and positioned emergence traps and plankton tows constitute a powerful combination in quantifying emergence behaviors and assessing their importance in benthic-pelagic coupling and in population dispersal.

## Methods

**Study area**—West Sound is a semienclosed inlet of Orcas Island in northern Puget Sound, Washington. It is ~2–2.5 km wide (east-west) and 4–5 km long (north-south), with typical depths of 20–25 m. The most precisely located site during our study in West Sound was the BAMS tower at 48°37.32'N, 122°58.36'W (average of many differential global positioning satellite fixes). The TAPS was deployed at 48°37.5'N, 122°57.9'W (fig. 1 of Self et al. 2001). At its mouth on the southern end, West Sound communicates with a narrow (~1 km wide) channel that experiences strong tidal flows. Mean current speed ( $\pm 1$  SD) 3 m above the bottom was  $2.4 \pm 1.6$  cm s<sup>-1</sup> measured nearby to TAPS (48°37.32'N, 122°58.36'W). West Sound was selected for the BAMS study because of its homogeneous, flat bottom. Its sediments consist largely of fine silt and clay (median grain size ~23  $\mu$ m). This bay and nearby East Sound have long been known to support very dense diatom populations in summer (Shelford 1935). They are excellent sites for acoustic studies of coastal biological processes because they are quiet, sheltered, and productive.

**Acoustic data collection**—The TAPS is a small (~65 cm long, 15.2 cm diameter), multiple-frequency, acoustic, zooplankton sensor (fig. 2 of Barans et al. 1997). We used it in an up-looking, echo-sounder mode at four frequencies, 265 and 420 kHz and 1.1 and 3.0 MHz, mounted on a steel frame resting on the bottom so that the faces of all four transducers faced upward and were ~80 cm above the bottom of the frame. The mounting frame sank into the mud during the course of the 6-d deployment. For purposes of analysis, we assume that the transducers were 12.5 cm above the seabed. Because of high turbidity and the fluidity of the sediment-water interface, the diver who retrieved it could not make the determination precisely, so the precision in our vertical placement is clearly overstated. We therefore report our results rounded to the nearest 0.1 m, consistent with the size of the range bins that we used. A 500-m, multiconductor cable served as a power supply for the TAPS and as a con-

duit for data transfer to a laptop computer ashore. The length of the available cable and the distance to an appropriate site for data acquisition precluded placing TAPS closer to the BAMS. Every 2 min, estimates of volume backscattering strength were obtained for 43 small volumes of the water column (bins) directly above TAPS, each 0.5 m thick. The half-power beam widths (-6 dB) for this implementation of the TAPS were nominally 5°. As a consequence of the conical shape of the beam, at 3 m above the TAPS the volume sampled was ~0.011 m<sup>3</sup>, whereas at 20 m it was 0.076 m<sup>3</sup>. Data collection began at 1548 h 26 July 1995 and ended at 1320 h 1 August 1995, for a total duration of 5.89 d. For data analyses, we used MATLAB 5.2 and 5.3 for the Macintosh (MathWorks 1997).

Each acoustic channel was sampled sequentially. Pulse lengths of transmissions were 336 ms, and echo envelopes were sampled every 168 ms beginning 168 ms after the end of pulse transmission until 172 samples were taken. Sound speed was assumed to be constant in the water column and calculated from in situ measurements of temperature, salinity, and pressure, using the method of Chen and Millero (1977). Within the TAPS, echo envelopes are detected, digitized, and squared; as set up for this particular deployment, summation of four consecutive samples resulted in estimates of volume scattering strengths with 0.5-m vertical resolution. The first 0.5-m bin was centered 0.4 m above the transducer, and the most distant was centered at 21.4 m. Because the TAPS settled into the mud bottom at a time and rate that is unknown, actual heights above the somewhat ill-defined bottom are not known with precision. Sinking of the frame into the mud may have caused bin heights to vary by up to 0.5 m. Because we know neither the time course nor the vertical extent of sinking, we made no attempt to correct for this "drift." Each frequency channel was sampled in rapid succession until each had been sampled 24 times. Values were accumulated (summed) for each frequency over the 24 samples within each fixed height bin. The 24 cycles took just under 2 min to complete; thus, after normalization, each output profile represented an average over ~2 min.

**Field sample collection, processing, and analysis**—During the study and after TAPS deployment, we collected emergence-trap samples from various locations in the study region. The trap was deployed for ~24-h periods beginning at midday times ranging from 1000 to 1400 h on 11, 18, and 24 August and 1, 8, 15, and 25 September 1995. It was pyramidal, enclosing 1 m<sup>2</sup> of seabed and standing 1 m high, with the faces of the pyramid covered in 1-mm Nitex netting. The base was made of aluminum angle stock to penetrate 2.5 cm into the sediment and seal off the trap. Two opposing corners each were loaded with 2-lb (907-g) diving weights to effect a seal. An inverted funnel at the top of the trap led through a 2-cm diameter tube into a collecting bottle. It was deployed by rope in upright position but with the collecting bottle removed. After it reached bottom, divers swam down the line and attached the sample bottle. The entire trap was retrieved by hoisting with the rope (tied off to a float during trapping) at the end of the deployment. Collected specimens both from these traps and later net hauls were fixed in 10%

formalin buffered with sodium tetraborate within several h after retrieval and transferred to 80% ethanol within 3 weeks.

Samples were sorted into broad taxonomic groups, and numbers of individuals in each group in each sample were counted. The groups were mysids, polychaetes (adult and juvenile), copepods, amphipods, decapod shrimp, cumaceans, ostracods, zoeae, megalopae, ctenophores, and medusae. Mysids in each sample were sorted by species. Only two species were present: *N. kadiakensis* and *Pacificanthomysis nephrothalma*. The total length (base of eyestalk to tip of telson) of each individual in each sample was measured under the dissecting microscope to the nearest millimeter, to support attempts to associate sizes determined acoustically with particular species and stages. Sexes of *N. kadiakensis* individuals in length classes >10 mm and of *P. nephrothalma* individuals in length classes >4 mm were determined with the aid of a dissecting microscope. Smaller individuals had no detectable or only rudimentary sexual characteristics and were classified as juveniles.

Mysids from different samples but of the same length class, sex, and species were then pooled into one group to make volume measurements. Average displacement volumes of individuals in a group were measured directly by submersion in a graduated cylinder containing 70% ethanol. Displacement volumes of mature females carrying young or eggs in marsupia may have been underestimated because of loss of some young from some marsupia during sample handling before submersion.

Volume-versus-length data obtained for the various species and sexes of mysids were used in model I (Sokal and Rohlf 1995), log-log regression. Because the 95% confidence intervals of both the slope and the intercept coefficients of regression overlapped between males and females of a species, we combined the data on males with the data on females of each species by taking the grand mean of the two sex-specific mean volumes at each size increment (before natural-log transformation). An *F*-test for the difference between the two regression slopes of volume versus length for *N. kadiakensis* and *P. nephrothalma* showed that they were different ( $P < 0.05$ ), so we did not combine them into a single curve.

A concern with the 1995 trap data, exacerbated by a lack of concurrent zooplankton tows, was the possibility that animals were trapped during the lowering through the water column. Additional emergence-trap samples therefore were collected during three 24-h periods (1000–1000 h) in mid-August 1997 (immediately following plankton tows). For lack of diver support and by means of a second tether, the trap was lowered inverted with the bottle in place, righted 3–4 m above the bottom, and then lowered the rest of the way. For comparison, four pairs of emergence-trap samples were also collected with diver support on consecutive days approximately weekly during September, deployed on 4, 5, 10, 11, 17, 18, 24, and 25 September. The first sample in each pair was collected as above and the second in upright mode (identical to the 1995 method) for comparison between the two methods. The 1997 emergence-trap samples were enumerated completely for the same varying broad taxonomic groups as in 1995 but with the addition of nauplii.

The acoustic data immediately suggested that an emergent

benthic population moved all the way to the surface, and all depth ranges of the water column exhibited greater back-scattering at night. We were interested in 1997 to assess whether compositional differences existed between the zooplankton of the two regions between night and day or if the two regions differed simply in concentrations of similar animals. From examination of the acoustic data, we selected two depths to perform zooplankton tows, one in the thick of the nighttime upper layer (2–3 m from the surface) and one through the center of the water column (~10 m). Daytime tows at the same depths would then serve as a baseline to see what taxa increased at night. The acoustics showed that ascent began ~2120 h, that vertical distribution was roughly stable by midnight, and that descent began sometime after 0400 or 0430 h. On the basis of these acoustic observations, we made the night plankton tows between 0030 and 0330 h and returned for the day tows from 1700 to 2000 h. Because this second sampling effort occurred 2 yr after the acoustic data were collected (albeit during the same month) and TAPS was no longer available, we were forced to assume that species presence or absence and behavior (general migration patterns) were similar in 1997 to 1995.

All tows were performed in the direction 120° south-southeast along a transect line that began in the immediate vicinity of the TAPS deployment and paralleled the 10.5-fathom (19.2-m) contour. We used a single, nonclosing zooplankton net with 0.5-m diameter circular mouth and a 500- $\mu$ m mesh. Day tows were made on 10, 12, and 14 August and night tows on 10, 13, and 14 August 1997. Estimated depth of the deeper tows was 6–11 m and of the shallower tows 1–3 m. Tow speed was about 4.3 km h<sup>-1</sup>. Three “replicate” 5-min tows were made consecutively at each depth. Samples were fixed within hours after capture in 4% formalin buffered with sodium tetraborate and transferred to 70% ethanol within 3 weeks. Mysids >8 mm (base of eyestalk to tip of telson) were sorted to species; other individuals of comparable size were sorted into major taxa, but the dense mixture of smaller animals, primarily crustaceans, was not separated.

Mann-Whitney *U*-tests compared day versus night catches at each depth, for all groups enumerated. Replicates at a depth and date were collapsed as a sum to satisfy independence; therefore, the sample size was limited to three nights, and it was impossible to obtain significance levels beyond  $P = 0.10$ . Nested ANOVA was used to obtain greater power where variances were (or could be transformed to be) homogeneous. Statistical analyses were carried out with SYSTAT 5.2.1 (Wilkinson et al. 1992), but the tests are also described in Sokal and Rohlf (1995).

*Processing to determine parameters of the migrations*—We pursued estimates of migration speeds and times of emergence and reentry with the 265-kHz data because this frequency exhibited the best signal-to-noise characteristics throughout the water column (Fig. 1). The data contained a number of discrete, high-intensity signals, at least some of which appeared to be echoes from individual, large scatterers—for example, from micronekton, large zooplankton, and fishes. For the purposes of the analyses related to migration speeds and times of emergence and reentry, we suppressed

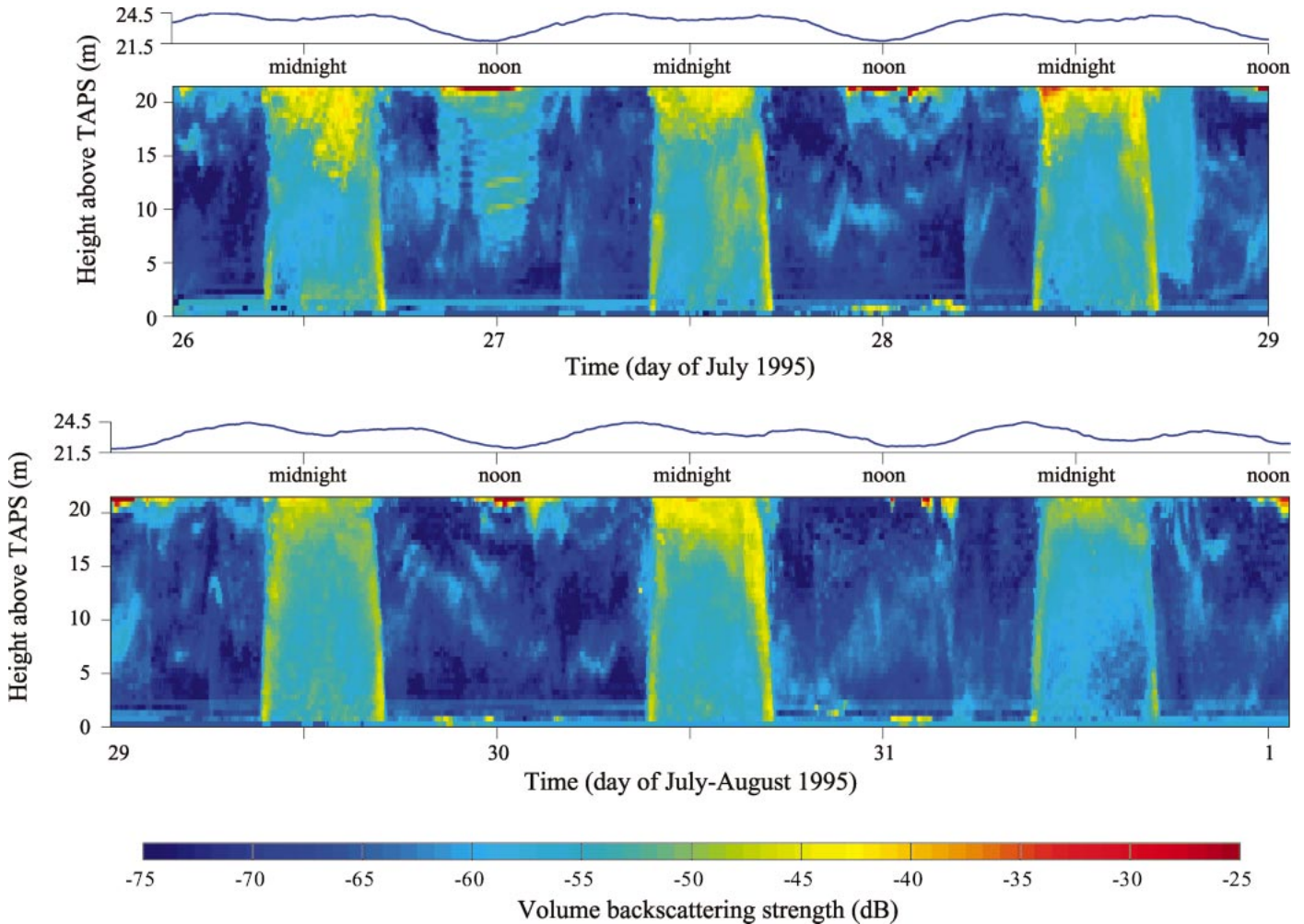


Fig. 1. The tidal record (blue curve) resulting from 11-point, running-mean smoothing of the pressure record from TAPS and volume backscattering strength at 265 kHz from TAPS. Time variation is dominated by the regular nightly sequences of emergence events. The midday, surface highs in apparent backscattering strength are artifacts from intersection of the beam with the air-sea interface as low tide brings it into the record. Native “pixels” are 2 min wide  $\times$  0.5 m tall, but this record has been smoothed (11-point running median), effecting a low-pass filter, simply because the 4,247 scans cannot be well resolved in the printed page size, even after splitting the record into two segments, as shown. Times are local (Pacific daylight savings time). The color scheme compresses all lower readings into the lowermost category ( $-75$  dB) and all higher readings into the uppermost category ( $-25$  dB).

the effects of these discrete echoes—that is, we smoothed over time rather than over depth intervals to preserve spatial precision. We explored several smoothing methods including a low-pass Butterworth filter, LOWESS (Cleveland 1979, 1981) and running medians. Running medians appeared to cause the least time distortion of ascents and descents and, being relatively insensitive to outliers, revealed “typical” values of the time series. We used 11-point running medians, sufficient to remove the spikiness apparent in the raw data but not so long as to blur significantly the migration events. Times of depth-specific maxima in backscatter intensity were obtained within 5-h intervals straddling each ascent and descent. Start and stop times of these 5-h intervals were shifted when emergence and reentry times were determined more objectively by regression, but this shift altered no results. Time of arrival of the leading edge of the emerging population in each bin (onset of increase) during ascents was

estimated by selecting the earliest time point in each bin series that was followed immediately by a threshold increase in a smoothed backscattering coefficient to a level  $\geq 5 \times 10^{-7} \text{ m}^{-1}$  ( $\geq -63$  dB). The exit of the trailing edge was defined by analogous criteria. Smoothing removed the effects of single, high scattering events, but a threshold was needed to eliminate spurious sensitivity to small patches of scatterers that occurred more randomly than the emergence events and were uncorrelated with preceding events above or below.

For the purposes of estimating group migration speeds, volume scattering data were truncated above 12.8 and below 1.8 m. Reverberation measurements were limited by low-level transducer ringing at short ranges, and heteroscedasticity (rapidly increasing variance with further height increase) precluded the use of longer ranges in our regressions. Thus, for each of the six nights, four sets of times were obtained

for each of the 22 depth bins in the truncated (11-m) measurement range, corresponding to onset of emergence, maximal backscattering from that bin during emergence, the maximum during reentry, and completion of reentry. We used the SYSTAT (version 5.2.1) MGLH module (Wilkinson et al. 1992) to do linear and curvilinear (second-order polynomial) regressions of time on height for each of the four profiles on each night to estimate group migration speed. Using linear regression forces constant migration speed, whereas a second-order polynomial forces constant acceleration. Ten points (<2% of the regression data) were removed as the most extreme statistical outliers on the basis of the ratio between the data range and the standard deviation (Dixon and Massey 1983), where the statistical population in question comprises the residuals from the regression fit.

Column scattering strength at 265 kHz (Medwin and Clay 1988) was integrated between 2.8 and 20.3 m to get some idea of the relative contribution of the emergent fauna. The bottom 2.3 m were excluded because of variability that we attribute to a combination of factors, possibly including sinking of the platform relative to the bottom, uncompensated transducer ringing, and gradual accumulation of fishes around the TAPS in an otherwise fairly unremarkable bottom topography. The data from the top 1.5 m of the scattering record were omitted to avoid periodic levels of high backscattering from the air-sea interface at the times of the low-low tides, which occurred between 1000 h near the beginning of the data collection period and 1300 h near the end of the experiment (Fig. 1). Data were divided into emergence and nonemergence periods on the basis of the regression-estimated times of emergence and reentry (defined by extrapolating intercepts of leading and trailing edges with the seabed).

*Acoustic estimation of the sizes and abundances of the migrators*—One of the advantages of using quantitative multifrequency acoustics is that it is often possible to extract estimates of both size and abundance from the measurements. Precision and accuracy of the estimates depend on the number of frequencies that one uses, the bandwidth over which the acoustic scattering are measured and the data quality (e.g., the reverberation-to-noise ratios at each acoustic frequency). It is also critical that the scattering models used in the calculations accurately reflect the frequency dependence of the actual scattering that one gets from the organisms that are in the water at the time and place of the measurements. The general methods for making these estimates have been extensively documented (e.g., Holliday 1977; Greenlaw and Johnson 1983; MacLennan and Simmonds 1992; Medwin and Clay 1998).

The data that we analyze herein were collected during the very first engineering tests of a TAPS in an echo-ranging mode. Although a number of technical problems were identified and later resolved, those issues affected our ability to use all of the collected data in a comprehensive inversion calculation. We therefore focused on the unexpectedly strong and regular migration patterns, which had not, to our knowledge, been previously observed with such high temporal and spatial resolution. We carefully selected segments of data for detailed analysis at times and depths where data quality at

multiple frequencies would support an inverse calculation. Examples of the issues that became apparent during our quality control were an unfortunate choice of system gain at 3 MHz, which largely precluded our use of that channel, except during a few short time intervals at limited ranges from TAPS. This problem was in part due to the unexpectedly high abundance of small particles that scattered at this frequency, location, and time of the year. Electronic noise in the time-varied gain circuitry, in turn, made the 420-kHz and 1.1-MHz returns unusable in the upper half of the water column, and mechanical transducer “ringing” plagued several depth bins nearest to TAPS on several channels. Nevertheless, we were able to find windows of usable data at intermediate distances from the bottom at all frequencies in each emergence and re-entry event. These windows consistently started at 5 m above TAPS. The extent of each analysis window varied between four and six depth bins (2–3 m) downward from 5 m in order to exclude short periods of low signal-to-reverberation measurements due to the transducer ringing on several channels. Usable time windows varied from 10 to 20 min and were based on the short durations of the transits through these small depth ranges.

Because mysids dominated the trap samples, we chose a distorted-wave Born approximation (DWBA) to calculate the scattering that one would expect from mysids of various sizes at the TAPS frequencies. This model has been used previously to describe scattering from elongate scatterers such as euphausiids (Chu et al. 1993; Stanton et al. 1993, 1998; Martin-Traykovski et al. 1998; McGehee et al. 1998). The DWBA method uses a digitized shape of the animal for which one wishes to calculate acoustic scattering. We used the digitized peripheral outline from a photograph of a mysid as the starting point for our calculations of the dependence of acoustic reflectivity from this animal shape on its size and the acoustic frequency. Details of the DWBA method, along with MATLAB code for calculating the scattering can be found in McGehee et al. (1998).

Sizes of the animals that appeared in the water column at dusk and reentered the benthic or hyperbenthic zone at daybreak were estimated by performing pixel-by-pixel inverse calculations during these emergence and reentry windows. Each pixel represented 2 min in time and 0.5 m in depth. The dozen emergence and reentry events yielded a total of 534 usable pixels. Size spectra across all these pixels were averaged, resulting in average biovolumes ( $\text{mm}^3 \text{m}^{-3}$ ).

*Other environmental data*—A Biospherical Instruments QCP-200A cosine photosynthetically active radiation (PAR) collector mounted on one leg of the BAMS tower at ~1 m above bottom recorded downwelling irradiance. Because the bottom sloped gently downward from the TAPS site toward the BAMS tower, this PAR sensor was at a water depth approximately equal to the bottom depth where TAPS was located. Ten measurements were taken over 50 s every 0.5 h on the half-hour and averaged. Data collection began at 0930 29 July 1995 and continued through September 1995. PAR and TAPS data overlapped for 3.04 d. The TAPS 100 psi pressure sensor mounted near the bottom of the frame recorded averaged pressures every 2 min for the duration of acoustic data collection, and they were converted to water

depth (Fig. 1). Mean tidal height above the sensor during data collection was 23.4 m, and tides ranged from 21.6 to 24.6 m. Temperatures were obtained from conductivity-temperature-depth (CTD) casts made with a custom Sea-Bird CTD (Seacat 19) on 29 and 30 July 1995 at 1209 and 1845 h, respectively, in the vicinity of BAMS.

Times of sunrise, sunset, twilight, moonrise, and moonset and the moon's phase in West Sound were obtained for the coordinates 48.6°N, 123.0°W from the U.S. Naval Observatory Astronomical Applications Department web page, <http://aa.usno.navy.mil/AA/data/> (the program having 0.1° resolution). Meteorological data were obtained from the nearest archival weather station on Smith Island (48.32°N, 122.84°W; <http://www.ndbc.noaa.gov>), ~37 km (20 nautical miles) south-southeast of the study site. Orographic channeling tends to make wind *direction* strongly dependent on nearby topography in the San Juan Archipelago. However, average wind *speeds* measured at Smith Island tend to be reasonably well correlated with those measured in East Sound, a few km from West Sound on Orcas Island (Dekshenieks et al. unpubl.). Archival wind data were obtained from <http://www.nodc.noaa.gov/BUOY/sisw1.htm>. Archival tide data were obtained from <http://www.tidesonline.nos.noaa.gov> for Friday Harbor, Washington. This tide station is located ~12 km (6.5 nm) south-southwest of the study site.

## Results and Discussion

*Variations in scattering with time, depth, and environmental variables*—Daily emergence and return clearly dominated time variation in the 6-d data set. The 265-kHz data revealed the nocturnal emergence and return most clearly and demonstrated that it originated either at or below the level of the sensor (Fig. 1). The 420-kHz channel (not shown) revealed a similar pattern in the lowermost half of the water column, where it returned reliable results. The most striking feature of the scattering pattern with time and depth (height above the TAPS) involved evening ascents, high nighttime volume scattering strengths ( $S_v$ ), and descents at dawn. Sudden, large increases in backscattering intensity from the near-bottom depth bins occurred shortly after dusk every evening, followed by increases in backscattering intensity at all levels in the water column. During the night, backscattering intensity was typically higher toward the surface than at greater depths, but all depths showed increased volume scattering over daytime levels. Before dawn a descent, crudely symmetrical with the ascent, occurred.

There was no overlap of emergence signal and positive PAR readings on our sensor. The major ascent began after light levels dropped below the instrument threshold of  $0.5 \times 10^{-6} \mu\text{mol quanta cm}^{-2} \text{s}^{-1}$ . Likewise, descent was complete and the trailing edge of the pulse passed below the transducer on all three nights before the PAR sensor again registered. Resolution was limited, however, not only by the threshold sensitivity of the meter but also by the sampling frequency for PAR (every 0.5 h). A new moon occurred on 27 July at 0814. The only day when the moon had risen for any interval after ascent (and before morning descent) was on 31 July, when it set at 2124 h and had 17% of its face

illuminated. Ascent occurred at 2119 h, so, because of the low angle of incidence, little moonlight could have entered the water. On other nights, moonset occurred before the ascent, so moonlight could not have affected either timing of emergence or between-night variances in the acoustic records.

Because the acoustic record was short, ascent always occurred on the minor ebb tide. The point in the tidal cycle when ascent began trended backward in the tidal cycle over the 6 days so that, whereas on the first night ascent began near mid ebb, on the last night it began near high slack. Descent occurred on the major ebb tide on the first two nights, near the time of high slack on the third night, and on the minor flood tide the last two nights. The repeatability of emergence times gives no reason to suspect strong tidal modulation of either emergence or reentry. More recent work in the Damariscotta estuary in Maine, however, shows much clearer modulation of the local mysid emergence by the much stronger tidal currents (Taylor and Jumars unpubl. data).

Temperatures were roughly constant through most of the water column (11–12°C), except for a thin, warm surface layer (13–16°C). The base of the thermocline was near 2–4 m depth during the period of the acoustic record. Backscattering records did not exhibit discernible structure near the thermocline.

Less intense and less regular variability in water column scattering was evident throughout the record. Patches, quasi-coherent layer structures, and scattering from “discrete” targets, as opposed to “volume” scattering appeared during both night and day as behavioral responses and advective processes modified the distribution of scatterers in the water column over the TAPS. Increases in  $S_v$  near times of lowest tides, but extending through much of the water column on the first day and decreasing in intensity and depth extent on subsequent days (as the height of the lowest tides gradually increased), are intriguing. Although strong, thin, scattering layers were occasionally observed during our occupation of the site in West Sound (Holliday et al. 1998), layered structures during this 6-d period were largely ephemeral and diffuse. Examination of the daylight periods (between migrations) in the scattering records of Fig. 1 reveals both patchiness and the presence of weak scattering layers that sometimes quickly changed depth with time.

Examination of the 265-kHz acoustic record from the daytime hours on 27 July (Fig. 1) reveals an increase in scattering near the surface, extending to ~6 m above bottom at midday, decreasing during the afternoon. It appears that two or three weak layers began to form, that they began to shoal as the water level rose with the incoming tide, and then either dissipated quickly or were advected away from the location of the TAPS. Weaker and shallower but otherwise similar features were observed during subsequent days, all at the times of slack water at the lowest tide of the day. On the first two days, 27 and 28 July, the lowest low tide and low winds, ~1 m s<sup>-1</sup>, coincided. On 29 July, wind speed dropped from near 20 m s<sup>-1</sup> earlier in the day to ~5 m s<sup>-1</sup> at the time of the lowest low tide. On 30 July, the winds peaked at ~7 m s<sup>-1</sup> at the time of the lowest low tide, and on the last full day of the acoustic record, 30 July, wind

speeds reached  $10 \text{ m s}^{-1}$  during the lowest low tide. At the beginning of the record this combination of low wind and slack water appear to have allowed the onset of weak water-column stratification, with an acoustically detectable zooplankton response during daytime.

*Acoustic inversion*—Because our primary physical samples came from emergence traps, we elected to restrict our inversion estimates to known emergence and reentry events most likely to be dominated by the same mysids caught in the traps. We had no clear basis, other than best fit, to choose inversion models for other times. It is reassuring, however, that the DWBA model for elongate scatterers such as mysids showed its best fit during emergence and reentry events and that a fluid-sphere inversion model often showed best fit at other times when other morphologies may have dominated (results not shown). For elongate scatterers, biovolume spectra calculated for the reentry phase of the migration were similar to those observed during emergence. Estimated biovolumes for elongate scatterers during the migrations were similar ( $4054 \text{ mm}^3 \text{ m}^{-3}$  in ascent vs.  $5197 \text{ mm}^3 \text{ m}^{-3}$  in descent).

*Times and speeds of ascents and descents*—A coarser-scale, single-frequency approach highlights the remarkable consistency in timing and speed of the dominant migrations from night to night (Fig. 2). Significant improvement of fit to the curvilinear model over the linear model (by *F*-test) for individual profiles was found in only two of six instances for onset of emergence, three of six for maximal backscattering during emergence, one of six for maximal backscattering during reentry, and three of six for completion of reentry. When present, curvature indicated deceleration during emergence and acceleration during reentry. Pooled profiles also were made by plotting all profiles against time relative to apparent emergence or reentry for the night in question. None of the pooled profiles was significantly curvilinear, however. We conclude that mild curvature (decelerating group velocity further in time and distance from emergence and reentry) was probably present but that linear regression captures most of the variance. Therefore we worked primarily with the linear regressions.

Slopes of the linear regressions were inverted to obtain estimates of population swimming speeds for the leading edge and mode of abundance of the population during ascent and the mode of abundance and trailing edge of the population during descent on each night. The time intercepts of the regression lines with  $z = 0$  provided estimates of times of onset of ascent and completion of descent in all four sets of profiles, corresponding to onset of emergence, maximal backscattering from that bin during emergence, the maximum during reentry, and completion of reentry (Table 1). The leading edge of the population ascended at  $0.0096 \pm 0.0025 \text{ m s}^{-1}$ ; the mode followed at  $0.0059 \pm 0.0024 \text{ m s}^{-1}$ . On descent, the mode of the population moved down at  $0.0067 \pm 0.0013 \text{ m s}^{-1}$ , followed by the trailing edge at  $0.0078 \pm 0.0014 \text{ m s}^{-1}$ . These SDs represent night-to-night variation in the least-squares slope estimates, not confidence limits based on individual nights' regressions. We avoided using the latter because the assumption that height-time

points in adjacent bins are independent is questionable. Two-sample *t* tests for equality of means, with the six nights in each column taken as six independent samples of a mean rate for that column, indicated no significant differences between ascent and descent speeds when compared using either the modes of the population ( $P > 0.4$ ) or the leading and trailing edges ( $P > 0.1$ ). Differences between the leading/trailing edge of the population and the mode were also insignificant for the descent ( $P > 0.1$ ) but were significant for ascent ( $P < 0.05$ ), with the leading edge moving faster. *F*-tests indicated no significant heteroscedasticity for any of the comparison pairs mentioned, although there is a tendency toward lower variance in descent speeds.

The six nights were taken as independent samples of emergence and reentry times. This assumption appears justified because horizontal advection by the tides virtually assures that individuals leaving one spot on the bottom after dusk will not return there at dawn. For that matter, the characteristic time to advect a patch of animals through the  $\sim 1.13\text{-m}$  diameter column of ensonified water is only 45 s ( $1.13 \text{ m}/0.025 \text{ m s}^{-1}$  characteristic tidal flow speed), making temporally adjacent acoustic profiles (2 min apart) more or less independent. That is, horizontal flow velocities typically are sufficient to clear each bin of its contents between adjacent sampling intervals (2 min apart). This point is important because it allows us with certainty to treat the 6 d of record as six independent realizations and therefore makes the regularity of migration even more impressive. The mean time of the beginning of emergence was 2116 h, with the mode following 14 min later. SDs of both of these times were 3 min. Modal reentry occurred at the bottom on average at 0504 h, and the mean time of completion of reentry followed by 14 min. These times both had SDs of 7 min. Although emergence appeared slightly more precisely timed than reentry, their variances were not quite statistically significantly different by *F* test ( $P = 0.1$ ). The leading edge of the population has reached a height  $\sim 8 \text{ m}$  above the bottom when the highest backscatter occurs near the bottom during emergence. Reentry is roughly symmetrical, the trailing edge being about 6.5 m off the seafloor when the greatest abundance reaches bottom (Fig. 2).

On some nights (e.g., Fig. 2, 26 July ascent), there was an apparent increase in near-surface backscattering at the same time as, or even preceding, the start of ascent near the bottom. We did not isolate the origin of this increase in backscatter. We cannot exclude the possibility that it originates from additional emergent individuals of the same or other species that do not show synchrony in emergence times, but it may originate as well from near-surface aggregation of holoplankton. In similar data collected in East Sound (Van Holliday unpubl. data), a slightly larger fjord located a few miles to the east on the same small island (Orcas Island), there was clear evidence that a reverse holoplankton migration was occurring at dusk and dawn during periods of minimal surface light at night (cloud cover or low levels of moonlight). Those data were collected in a way that allowed one to observe the surface during the entire tidal cycle. A part of the nighttime increase in scattering near the surface was clearly due to movement of organisms that lived very near the surface (neuston) to locations deeper in the water

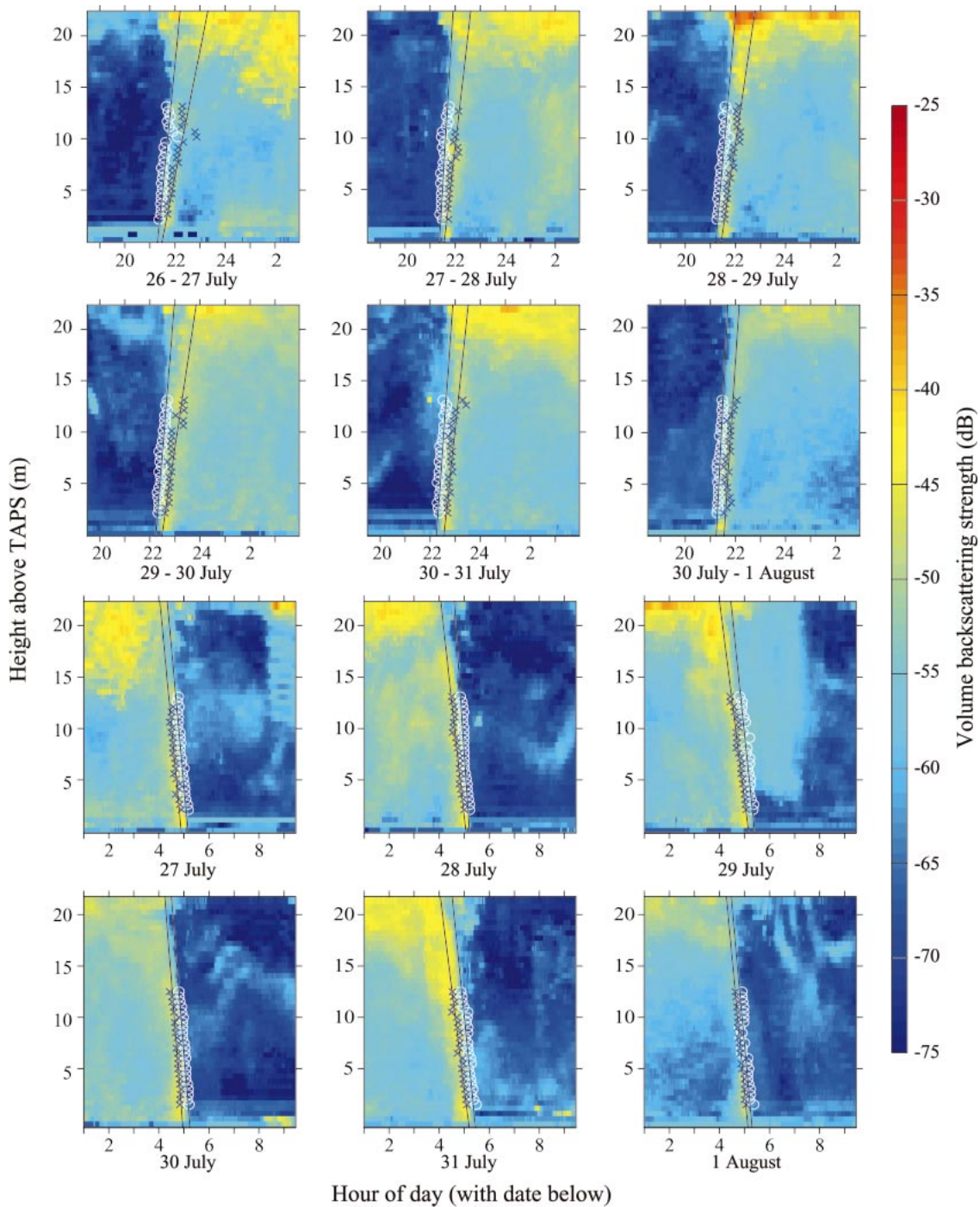


Fig. 2. Linear regressions on 11-point, median-smoothed backscattering coefficients for the 265-kHz data at each height in a band of heights near the bottom, to determine times (intercepts with the seabed) and speeds (slopes) of emergence and return. These parameters are calculated in two ways for each event. Leading edges of the migration are regressed, respectively, as the first (emergence) or last (return) pixels above background levels at that height (white circles). Maximal backscattering during the emergence or return (blue  $\times$  marks) is a better reflection of the modal tendencies of the population, but both figures represent average velocities of groups of individuals, because horizontal current speeds exceed by a factor of 2 the observed vertical migration speeds. Note the variations from day to day and the suggestions of other migrations within the time spanned by the major one treated by the regression.



Table 1. Group ascent and descent speed statistics (all in  $\text{m s}^{-1} \times 10^{-3}$ ) calculated from the regressions of Fig. 3.

Statistic	Ascents		Descents	
	Leading edge	Center	Center	Trailing edge
Night 1	6.9	3.4	7.3	7.5
Night 2	11.2	5.9	6.2	10.3
Night 3	7.9	4.6	5.4	6.6
Night 4	8.4	4.6	8.7	8.4
Night 5	9.5	6.4	5.4	6.7
Night 6	13.7	10.2	7.2	7.5
Mean	9.6	5.9	6.7	7.8
Standard deviation	2.5	2.4	1.3	1.4

column during the night. This kind of planktonic response to light (a reverse migration) has been reported for *Pseudocalanus* spp. in Dabob Bay, an arm of southern Puget Sound (Ohman et al. 1983; Ohman 1990). *Pseudocalanus* is a small (millimeter-sized) copepod commonly found throughout Puget Sound and was collected in both 1996 and 1998 in East Sound. It is possible that mysid emergence would drive such a reverse migration.

Estimated group migration speeds of scatterers ( $0.34\text{--}1.37 \text{ cm s}^{-1}$ ) are generally less than one body length per second for the mysids captured and are much slower than the maximal swimming speeds and even normal cruising speeds of individuals. Some mysids can attain swimming speeds  $>20\text{--}30$  body lengths  $\text{s}^{-1}$  (Mauchline 1980). During normal cruising, achieved by rhythmic beating of the thoracic exopodites, speeds are slower. *Mysis relicta*, a lake species of similar size to the elongate scatterers that we observed, has been the subject of many diurnal vertical migration and light-response studies. Its normal swimming speeds in the field have been estimated at  $0.02\text{--}0.05 \text{ m s}^{-1}$  (Bowers et al. 1990); additionally, Wong et al. (1986) found cruising speeds of  $0.005\text{--}0.032 \text{ m s}^{-1}$  in the laboratory. A model of the scatterer population of mysids swimming rapidly upward after an environmental cue has triggered the behavior is not supported. The slow speeds may suggest that ascent and descent are tightly regulated by ambient light intensities in the water column, although we lack the resolution in time and intensity of the wavelengths of light near 515 or 520 nm to which mysids are sensitive (e.g., Herman 1962; Gal et al. 1999) to test specific hypotheses about the movement with respect to in situ light (see Boden and Kampa 1967; Teraguchi et al. 1975).

Acoustic estimates of population swimming speeds during vertical migration have been made for both deep and shallow scattering layers composed of mysids and other scattering taxa. Teraguchi et al. (1975) found that most displacements of the leading edge of a population of *M. relicta* on a 200-kHz echogram in 50 m of water in a lake fell in the  $0.0\text{--}0.008 \text{ m s}^{-1}$  range during both ascent and descent over eight nights of measurements spanning 5 months. The distribution of group swimming speeds on ascent, however, tended toward higher values in summer than in late fall.

Onset of ascent as well as completion of descent in our data varied remarkably little night to night ( $\text{SD} \sim 3 \text{ min}$  for

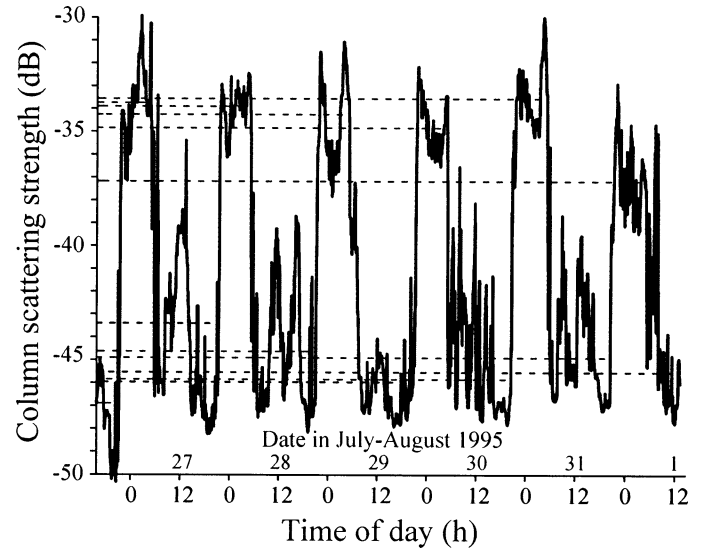


Fig. 3. Eleven-point (22-min) smoothed column scattering strengths (in dB) at 265 kHz over the duration of the observations. Horizontal dotted lines connect the ordinate with the median (unsmoothed) value of column strength during each emergence and nonemergence interval, revealing a 14-fold (11.46 dB) difference between the median of medians for the nocturnal emergence periods versus the median of medians for the nonemergence periods.

ascents and 7 min for descents). The spread of the times that the individuals in the migratory population leave (and return to) the bottom, as seen in the width of the pulse, however, is on any given night larger (estimated range, 30–40 min). This observed pattern could result from different individuals being adapted to respond to changes in the environment differently (i.e., to respond to different environmental cues or different levels of cues) or from night-to-night variability in individual response relative to the same cue (which is assumed to have occurred at nearly the same time each night during the short study period). As an example, DeRobertis et al. (2000) observed that small individuals led the upward and lagged the downward migration of a population of euphausiids in Saanich Inlet, British Columbia. At the other extreme, the variance of ascent-descent times in the population seen in the acoustics could be equaled by the night-to-night variances within individuals, perhaps as a function of varying feeding conditions and chemical cues from predators.

Ascent and descent are roughly symmetrical in space and time by estimates of our analysis. There were no significant differences in rates of vertical movement in the two directions. Given that the physiological state of the average migrator and that the reason for migrating is likely to be different at dusk than at dawn, one might expect average swimming speeds to be different during ascent and descent. Also, the direction of gravity's pull is reversed, and passive sinking is a potential addition to downward movement and impeding to upward swimming. Furthermore, the descent appears to be more coherent near the bottom than at the surface, like the ascent. If an ascent or descent were triggered and not controlled after the trigger, the forms of ascent and descent should be the vertical reverse of each other. That

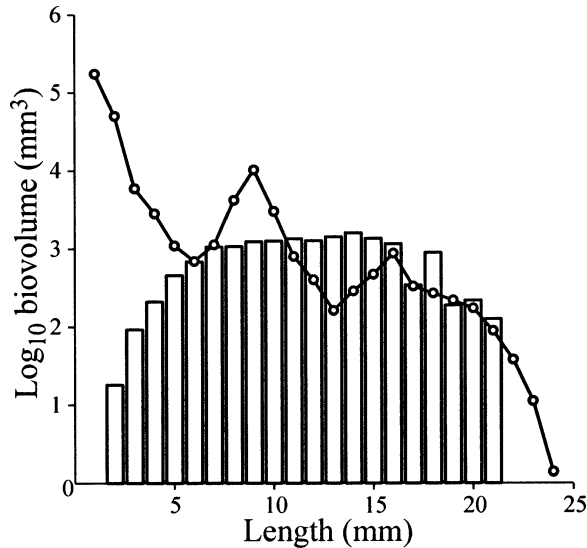


Fig. 4. Bars illustrate the biovolume-size spectrum for the pooled collection of all mysids from the seven 1995 emergence traps and so would carry unusual units [ $\text{mm}^3 (7 \text{ m}^2)^{-1} \text{d}^{-1}$ ]. Because the height of the bars is thus rather arbitrary, only the shape of the distribution should receive much attention. The line displays the cumulative size spectrum derived from acoustic volume scattering strengths collected and pooled over all 12 of the emergence and return events of Fig. 2, and the ordinate is in units of  $\text{mm}^3 \text{m}^{-3}$ . For the emergence-trap data, the SD at each size was approximately equal to the mean. Size ranges occupied by the trap-captured mysid population roughly match acoustic estimates of the size spectra for the entire assemblage of elongate organisms in the emergence events, departing at the high and low size extremes likely due to trap bias (see text).

rates of vertical net population movement during migration were slower than maximal swimming rates of mysids and that the ascent and descent were symmetric in speed, form, time-spread, and variance lends some weak support to the idea that the migrations are controlled by light and are not a result of an “all-or-nothing” response after a trigger; light is a symmetrical cue.

In addition to the scatterers that ascend to the upper water column, some occupy various positions through the entire water column during the night. This spreading is a well-known form of migration in coastal mysids (Mauchline 1980). Additionally, many studies of mysids have found a portion of the population on the bottom at night. Mauchline (1980), however, points out that there may be a continuous interchange of individuals, upward and downward, within the vertical structure of the population, so that it is unclear whether animals captured on the bottom have indeed spent all night there. Thus, the distribution seen in the acoustic data could be due to more-or-less continuous change in vertical position of individuals or to individual differences in height selection. *N. kadiakensis* shows some between-habitat variability in behavior as well. Thorne (1968) found that it migrated to the bottom in Port Orchard, Washington, but not in deeper Case Inlet, Washington. The animals we observed acoustically must have been concentrated in the lowest 0.5 m of water or in the bottom during the day, consistent with

Clutter's (1967) observations that *N. kadiakensis* is hypopelagic during the day, staying within 30 cm of the seabed.

Additionally, some features indicate night-to-night variability in the time of highest buildup in backscatter in the lower portion of the water column during the night. Sometimes, there appears to be a second migratory wave from the bottom (Fig. 2). Alldredge and King (1980) found that some amphipods delay emergence until moonset and return to the seabed at moonrise. We do not have enough data to draw conclusions about thermal inhibition or tidal modulation of emergence, but it is clear that high-resolution acoustic technologies could provide useful longer-term information on the response of the benthopelagic community to these environmental stimuli and constraints.

Emergence dominated not only time variation in the record, but also backscatter intensity. The usable depth interval showed a difference of 11.46 dB between medians of medians (Fig. 3) during emergence events versus during the periods between emergence events. Decibels are relative measures of backscattering intensity; by definition, 10 times the  $\log_{10}$  of the ratio in column backscattering strength (emergence/nonemergence) equals 11.46. Solving for the ratio yields the conclusion that column scattering strength is 14 times higher during emergence events. At 265 kHz, then, emergers grossly dominate the holoplankton in their effects on backscatter.

*Emergence-trap collections*—As the discussion to this point has anticipated, in the 1995 traps, mysids were by far the most abundant group enumerated, constituting 93% of the total catch by numbers. Cumaceans also were present in the trap samples, as well as medusae, megalopae, ctenophores, zoeae, and copepods. Some of these organisms, occurring in low numbers, were captured consistently in daytime plankton tows and are considered to be planktonic contaminants: ctenophores, zoea, megalopae, medusae, and some types of copepods. Two species of mysids occurred in the samples, *N. kadiakensis* and *P. nephrophthalma*. *N. kadiakensis* dominated. A broad size spectrum of mysids was captured (Fig. 4), from juveniles just larger than the final larval stage of their species to large, mature females approaching the largest sizes reported for their species (Kathman et al. 1986). In the trap samples, mysids were ~54 times more numerous than the next most abundant group, the amphipods. Constitution of the aggregate size-frequency spectrum obtained by acoustic inversion potentially violates assumptions of statistical independence by using groups of adjacent pixels, and emergence-trap samples do the same by capturing animals from the same square meter of seabed, but the good match in size frequencies by the two methods (Fig. 4) is one more piece of evidence that mysids indeed are principal sources of the emergence signatures seen acoustically (Figs. 1–3). Departures of the two methods at the small end probably reflect undersampling due to the mesh size of the trap, whereas departures at the large end probably reflect the rarity of large individuals that are undersampled by the trap either due to their rarity and the small sample size or to their effective avoidance behaviors (or both).

Mysids were also most abundant of the taxa captured in the 1997 emergence traps, but not as strongly dominant as

in 1995, constituting only 42% of the total catch. Emergence of the polychaete *Scalibregma inflatum* was captured on 10–11 September, 1 d after the first quarter moon. This reproductive swarming behavior has been noted elsewhere in this species (Fage and Legendre 1927). Copepods were captured in much greater numbers than in 1995, and several benthic genera were present.

*Plankton net-tow collections*—In the 1997 plankton tows, only seven of the enumerated taxa suggested significant differences in vertical distribution from day to night ( $P < 0.10$ , Mann-Whitney  $U$  test). They were *N. kadiakensis* juveniles, females, and males; fishes; bivalves; ctenophores; and megalopae of *Cancer magister*. No *Neomysis* individual was captured in any of the 18 daytime tows, but as many as 176 were captured in deep, nighttime hauls. Bivalves had a higher daytime mean at the deeper depth, whereas the rest had higher nighttime means. We suspect that the deep tows (at least during the day, perhaps dependent on the currents) scraped the bottom because bivalves were captured in seven of nine deep daytime tows, and mud was present on the net in two of those samples. A lone bivalve was also captured in a shallow night tow once.

Ctenophores (all *Pleurobrachia bachei*) were significantly more abundant in night tows than the day at both depths by ANOVA with  $P < 0.05$  at the shallow depth and  $< 0.001$  at the deep depth. Megalopae (*C. magister*) also appear to be migrating, showing a minimum 13-fold nighttime increase of mean abundance in all day-night comparisons in the shallow depth. Although it is possible that these two taxa contributed to the acoustic patterns seen at night, they were not part of the population emerging from below 0.5 m above the substrate. That some groups failed to show significant day-night differences between sample depths does not allow us to conclude that they were not migrating. Rather, it reflects the rarity of their capture and arbitrary choice of sampling depths. Many other important groups were not enumerated, such as the amphipods and copepods. Of the six large (20–35 mm) decapod shrimp captured (*Crangonidae*, *Hippolytidae*, and *Pandalidae*), all were caught in the deep depths, and five were captured at night. Of the 147 individual mysids of six other species, 145 were caught at night. Trap and net data both provide a consistent picture of nightly emergence by macroscopic shrimp at this site.

In summary, the high resolution of acoustic data offers excellent potential for testing behavioral hypotheses and for correlating spatiotemporal patterns with other environmental data. Using acoustic information to choose times and places for “surgical” placement of physical (net or trap) samples is an efficient means to accelerate analysis of the complex migration patterns already known in shallow-water communities (e.g., Takahashi and Kawaguchi 1997). Analogous forces of selection to those that have driven daily migrations of deep scattering layers in the open sea likely have driven daily migrations into the bottom or into turbid, near-bottom layers in shallow water, and such migrations are probably more common and spatially coherent than non-acoustic sampling has revealed. Mysids are ubiquitous in nearshore, boreal communities and are major components in the diets of many fishes (Mauchline 1980). Implications for bioturbation,

benthic community structure and the near-seabed acoustic environment are substantial, just as they are for material exchanges between benthic, planktonic and nektonic components of nearshore ecosystems.

## References

- ALLDREDGE, A. L., AND J. M. KING. 1980. Effects of moonlight on the vertical migration patterns of demersal zooplankton. *J. Exp. Mar. Biol. Ecol.* **44**: 133–156.
- BARANS, C. A., B. V. STENDER, D. V. HOLLIDAY, AND C. F. GREENLAW. 1997. Variation in the vertical distribution of zooplankton and fine particles in an estuarine inlet of South Carolina. *Estuaries* **20**: 467–482.
- BODEN, B. P., AND E. M. KAMPA. 1967. The influence of light on the vertical migrations of an animal community in the sea. *Symp. Zool. Soc. Lond.* **19**: 15–26.
- BOWERS, J. A., W. E. COOPER, AND D. J. HALL. 1990. Midwater and epibenthic behaviors of *Mysis relicta* Loven: Observations from the Johnson-Sea-Link II submersible in Lake Superior and from a remotely operated vehicle in northern Lake Michigan. *J. Plankton Res.* **12**: 1279–1286.
- CHEN, C. T., AND F. J. MILLERO. 1977. Speed of sound in seawater at high pressures. *J. Acoust. Soc. Am.* **62**: 1129–1135.
- CHU, D., K. G. FOOTE, AND T. K. STANTON. 1993. Further analysis of target strength measurements of Antarctic krill at 38 and 120 kHz: Comparison with deformed cylinder model and inference of orientation distribution. *J. Acoust. Soc. Am.* **93**: 2985–2988.
- CLEVELAND, W. S. 1979. Robust locally weighted regression and smoothing scatterplots. *J. Am. Stat. Assoc.* **74**: 829–836.
- . 1981. LOWESS: A program for smoothing scatterplots by robust locally weighted regression. *Am. Stat.* **35**: 54.
- CLUTTER, R. I. 1967. Zonation of nearshore mysids. *Ecology* **48**: 200–208.
- DEROBERTIS, A., J. S. JAFFE, AND M. D. OHMAN. 2000. Size-dependent visual predation and the timing of vertical migration in zooplankton. *Limnol. Oceanogr.* **45**: 1838–1844.
- DIXON, W. J., AND F. J. MASSEY. 1983. *Introduction to statistical analysis*, 4th ed. McGraw-Hill.
- FAGE, L., AND R. LEGENDRE. 1927. Pêches planctoniques à la lumière, effectuées à Banyuls-sur-Mer et à Concarneau. I. Annelides Polychètes. *Arch. Zool. Exp. Gén.* **67**: 23–222.
- FARQUHAR, G. B. [ED.]. 1970. Proceedings of an international symposium on biological sound scattering in the ocean. Maury Center Report 005. U.S. Naval Oceanographic Office, U.S. Government Printing Office.
- GAL, G., E. R. LOEW, L. G. RUDSTAM, AND A. M. MOHAMMADIAN. 1999. Light and diel vertical migration: Spectral sensitivity and light avoidance by *Mysis relicta*. *Can. J. Fish. Aquat. Sci.* **56**: 311–322.
- GREENLAW, C. F., AND R. K. JOHNSON. 1983. Multiple-frequency acoustical estimation. *Biol. Oceanogr.* **2**: 227–252.
- HERMAN, S. S. 1962. Spectral sensitivity and phototaxis in the opossum shrimp *Neomysis americana* Smith. *Biol. Bull.* **123**: 562–570.
- HOLLIDAY, D. V. 1977. Extracting bio-physical information from the acoustic signatures of marine organisms, p. 619–624. In N. R. Anderson and B. J. Zahuranec [eds.], *Ocean sound scattering and prediction*. Plenum.
- . 1993. Zooplankton acoustics, p. 733–740. In B. N. Desai [ed.], *Oceanography of the Indian Ocean*. Balkema.
- , R. E. PIEPER, C. F. GREENLAW, AND J. K. DAWSON. 1998. Acoustical sensing of small-scale vertical structures in zooplankton assemblages. *Oceanography* **11**: 18–23.

- JACKSON, D. R., AND K. B. BRIGGS. 1992. High-frequency bottom backscattering: Roughness versus sediment volume scattering. *J. Acoust. Soc. Am.* **92**: 962–977.
- JUMARS, P. A., D. R. JACKSON, T. F. GROSS, AND C. SHERWOOD. 1996. Acoustic remote sensing of benthic activity: A statistical approach. *Limnol. Oceanogr.* **41**: 1220–1241.
- KATHMAN, R. D., W. C. AUSTIN, J. C. SALTMAN, AND J. D. FULTON. 1986. Identification manual to the Mysidacea and Euphausacea of the northeast Pacific. *Can. Spec. Publ. Fish. Aqu. Sci.* **93**: 1–411.
- MATHWORKS. 1997. MATLAB: The language of technical computing. MathWorks.
- MACLENNAN, D. N., AND E. J. SIMMONDS. 1992. Fisheries acoustics. Chapman and Hall.
- MARTIN-TRAYKOVSKI, L. V., R. L. O'DRISCOLL, AND D. E. MCGEHEE. 1988. Effect of orientation on broadband acoustic scattering of Antarctic krill *Euphausia superba*: Implications for inverting zooplankton spectral acoustic signatures for angle of orientation. *J. Acoust. Soc. Am.* **103**: 236–253.
- MAUCLINE, J. 1980. The biology of mysids and euphausiids. *Adv. Mar. Biol.* **18**: 1–680.
- MCGEHEE, D. E., R. L. O'DRISCOLL, AND L. V. MARTIN-TRAYKOVSKI. 1998. Effects of orientation on acoustic scattering from Antarctic krill at 120 kHz. *Deep-Sea Res. II* **45**: 1273–1294.
- MEDWIN, H., AND C. S. CLAY. 1998. Fundamentals of acoustical oceanography. Academic.
- OHMAN, M. D. 1990. The demographic benefits of diel vertical migration by zooplankton. *Ecol. Monogr.* **60**: 257–281.
- , B. W. FROST, AND E. B. COHEN. 1983. Reverse diel vertical migration: An escape from invertebrate predators. *Science* **220**: 1404–1407.
- SELF, R. F. L., P. A'HEARN, P. A. JUMARS, D. R. JACKSON, M. D. RICHARDSON, AND K. B. BRIGGS. 2001. Effects of macrofauna on acoustic backscatter from the seabed: Field manipulations in West Sound, Orcas Island, WA, USA. *J. Mar. Res.* **59**: 991–1020.
- SHELFORD, V. E. 1935. The major communities. Pt. I Some marine biotic communities of the Pacific coast of North America. *Ecol. Monogr.* **5**: 251–292.
- SOKAL, R. R., AND F. J. ROHLF. 1995. Biometry. Freeman.
- STANTON, T. K., D. CHU, AND P. H. WIEBE. 1998. Sound scattering by several zooplankton groups. II. Scattering models. *J. Acoust. Soc. Am.* **103**: 236–253.
- , ———, ———, AND C. S. CLAY. 1993. Average echoes from randomly oriented random-length finite cylinders: Zooplankton models. *J. Acoust. Soc. Am.* **94**: 3463–3472.
- TAKAHASHI, K., AND K. KAWAGUCHI. 1997. Diel and tidal migrations of the sand-burrowing mysids, *Archaeomysis kokuboi*, *A. japonica* and *Iella ohshimai*, in Otsuchi Bay, northeastern Japan. *Mar. Ecol. Prog. Ser.* **148**: 95–107.
- TERAGUCHI, M., A. D. HASLER, AND A. M. BEETON. 1975. Seasonal changes in the response of *Mysis relicta* Loven to illumination. *Verh. Int. Ver. Limnol.* **19**: 2989–3000.
- THORNE, R. E. 1968. Diel variations in distribution and feeding behavior of Mysidacea in Puget Sound. M.S. thesis, Univ. of Washington.
- TREVORROW, M. V., AND Y. TANAKA. 1997. Acoustic and in situ measurements of freshwater amphipods (*Jesogammarus anandalei*) in Lake Biwa, Japan. *Limnol. Oceanogr.* **42**: 121–132.
- WILKINSON, L., M. HILL, AND E. VANG [EDS.]. 1992. SYSTAT: Statistics, version 5.2 ed. SYSTAT.
- WONG, C. K., C. W. RAMCHARAN, AND W. G. SPRULES. 1986. Behavioral responses of a herbivorous calanoid copepod to the presence of other zooplankton. *Can. J. Zool.* **64**: 1422–1425.

Received: 22 March 2002  
 Accepted: 25 November 2002  
 Amended: 9 December 2002